Journal of Catalysis 258 (2008) 250–255

Contents lists available at ScienceDirect

Journal of Catalysis

www.elsevier.com/locate/jcat

One-step conversion of acetone to methyl isobutyl ketone over Pd-mixed oxide catalysts prepared from novel layered double hydroxides

Robert D. Hetterley, Richard Mackey, James T.A. Jones, Yaroslav Z. Khimyak, Andrew M. Fogg, Ivan V. Kozhevnikov *

Department of Chemistry, University of Liverpool, Liverpool L69 7ZD, United Kingdom

ARTICLE INFO

Article history:
Received 26 February 2008
Revised 12 June 2008
Accepted 12 June 2008
Available online 11 July 2008

Keywords:
Methyl isobutyl ketone
Acetone
Palladium
Layered double hydroxides
Catalysis

ABSTRACT

Novel layered double hydroxides, $[MAl_4(OH)_{12}](NO_3)_2{\cdot}nH_2O$ ($M = (Li^+)_2$, Co^{2+}, Ni^{2+}, Cu^{2+}, Zn^{2+}), impregnated with palladium, have proved to be precursors to active bifunctional mixed oxide catalysts for the one-step synthesis of methyl isobutyl ketone (MIBK) from acetone and H_2 in the gas phase. High acetone conversions of up to 76% and MIBK selectivities of up to 91% were recorded at a reaction temperature of 250 °C and atmospheric pressure. The palladium catalysts based on Li and Zn layered double hydroxides displayed efficient catalytic performances at the low reaction temperature of 120 °C. Powder XRD and ^{27}Al MAS NMR showed that initially crystalline layered double hydroxides transformed to amorphous mixed oxide materials upon catalyst activation at 250 °C under H_2.

1. Introduction

Methyl isobutyl ketone (MIBK) is produced on industrial scale to be used mainly as a solvent in paints, coatings and resins. The industrial production of MIBK has generally employed a three stage process involving the base-catalysed aldol condensation of acetone to produce diacetone alcohol (DA), the acid-catalysed dehydration of the DA to mesityl oxide (MO) and the metal-catalysed (e.g. Ni, Cu, Pd) hydrogenation of MO to MIBK (Scheme 1) [1]. The use of homogeneous base and acid catalysts creates the problem of significant amounts of salt waste from catalyst neutralisation in addition to corrosion problems. Heterogeneous multifunctional catalysts that contain acid–base and metal functionalities and therefore capable of carrying out all three reactions in a single step in the liquid or gas phase without separation of the intermediate DA and MO have attracted considerable interest. Heterogeneous catalysts also have the advantage of being reusable, with the possibility of regeneration. In one-step synthesis of MIBK, diisobutyl ketone (DIBK) also forms in further reactions of MIBK as a useful byproduct which is a good solvent for a variety of natural and synthetic resins. Palladium is predominantly used as the hydrogenation component in the multifunctional catalysts for the reaction because of its high activity and selectivity for hydrogenating the C=C bond rather than the C=O bond [2]. One-step systems employing heterogeneous bifunctional catalysts such as Pd-doped strong acidic resin and Pd supported on zirconium phosphates have been used industrially in liquid phase at 120–160 °C and 20–50 bar H_2 pressure to achieve MIBK selectivities of up to 95% at 30–40% acetone conversion [1]. High operating pressure is an obvious disadvantage and adds significantly to the total production cost. Therefore much work has now been put into developing catalysts for the one-step process to be performed at atmospheric pressure in the gas phase. Catalysts used in the one-step MIBK production at atmospheric pressure include palladium supported on heteropoly acid [3], Zn–Cr mixed oxides [4], zeolites (ZSM-5 [5], faujasites X and Y [6], $AlPO_4$-11 and SAPO-11 [7]). Reaction temperatures range from 100–300 °C, with selectivities to MIBK generally lower in a gas-phase fixed-bed reactor than in a liquid-phase batch reactor. Catalyst deactivation is generally a problem as well.

Layered double hydroxides (LDHs), also known as anionic clays and hydrotalcites, have numerous applications in heterogeneous catalysis as catalysts or catalyst precursors [8,9]. LDHs were first synthesised in 1973 and have the general formula $[M^{z+}_{1-x}M^{3+}_x(OH)_2]^{b+}[A^{n-}_{b/n}]{\cdot}mH_2O$, where M^{z+} is a divalent or monovalent cation and A^{n-} is the interlayer anion [10]. Since that initial report there have been numerous synthetic studies into the LDHs and several reviews describing their composition have been published [8,11,12]. They can be thought of as structurally derived from brucite ($Mg(OH)_2$) like layers, where magnesium ions are surrounded approximately octahedrally by hydroxide ions [13]. Layers are formed by the octahedra edge-sharing, creating two dimensional sheets that stack together to form three-dimensional structures through hydrogen bonding. Some of the divalent cations in LDHs are substituted by trivalent cations, giving the layers a net positive charge which is balanced by the intercalation of various anions, e.g. NO_3^-, Cl^-, SO_4^{2-}, sulfonates, carboxylates, as well as wa-

* Corresponding author. Fax: +44 151 794 3588.
E-mail address: I.V.Kozhevnikov@liverpool.ac.uk (I.V. Kozhevnikov).

0021-9517/$ – see front matter
doi:10.1016/j.jcat.2008.06.017

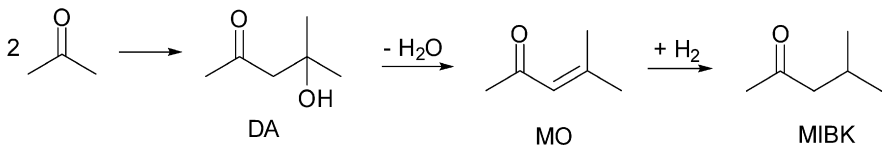

Scheme 1. MIBK synthesis from acetone and H_2.

ter molecules, between the layers. The catalytic properties of LDHs were first reported by Reichle in 1985 [14], and since then there have been numerous other studies [8,9]. Brucite-like Mg/Al LDHs containing Ni^{2+}, Co^{2+} or Fe^{2+} [15] and Pd-doped Mg/Al LDHs (hydrotalcites) [16–20] have been reported to be catalyst precursors in the synthesis of MIBK in gas-phase reactions at atmospheric pressure and liquid-phase reactions at higher pressures. Within these studies, the LDH structure is converted into active Mg/Al mixed oxide catalysts containing both acid and basic sites by calcination at temperatures of 350–500 °C.

Recently a new family of layered double hydroxides $[MAl_4(OH)_{12}][NO_3]_2{\cdot}nH_2O$ ($M = (Li^+)_2$, Co^{2+}, Ni^{2+}, Cu^{2+}, Zn^{2+}) has been synthesised based on the intercalation of metal cations into the octahedral holes of gibbsite γ-$Al(OH)_3$ [21–23]. The metal cations can be either divalent, forming $[MAl_4(OH)_{12}][NO_3]_2{\cdot}nH_2O$ where $M^{2+} = Zn^{2+}$, Co^{2+}, Ni^{2+} and Cu^{2+}, or monovalent, e.g. Li^+, forming $[LiAl_2(OH)_6][NO_3]{\cdot}nH_2O$. These materials have a very different layer composition and anion exchange capacity when compared to the brucite-like materials. Mechanistic studies on the formation of the gibbsite intercalates using time resolved in situ energy dispersive X-ray diffraction have shown that they form via a direct intercalation process rather than via dissolution/reprecipitation mechanism [24,25]. It is these materials, which are derived from gibbsite, that are the focus of our study. This paper describes the one-step conversion of acetone to MIBK in the gas phase over Pd-doped mixed oxide catalysts prepared from these novel layered double hydroxides and represents the first report of catalytic activity observed for the divalent metal cation intercalates of gibbsite.

2. Experimental

2.1. Catalyst preparation

The $[MAl_4(OH)_{12}][NO_3]_2{\cdot}nH_2O$ ($M^{2+} = Co^{2+}$, Ni^{2+}, Cu^{2+} and Zn^{2+}) LDHs were prepared as reported by Fogg et al. [22]. The gibbsite was activated in a ball mill for several days then treated hydrothermally with a 10 M metal nitrate solution at 150 °C for 48 h. $[LiAl_2(OH)_6][NO_3]{\cdot}nH_2O$ and $[LiAl_2(OH)_6][OH]{\cdot}nH_2O$ were prepared by the direct reaction of lithium salts in aqueous solution with unactivated gibbsite at 90 °C overnight. Pd-loaded layered double hydroxides were prepared by impregnating ground LDH with $Pd(OAc)_2$ in benzene suspension followed by reduction of Pd^{2+} to Pd^0 in H_2 flow at 250 °C for 2 h [4]. During the reduction, the structure of LDH collapsed losing structural water and the interlayer nitrate or hydroxide anions to form a mixed oxide. The Pd loading in the resulting mixed oxide catalysts was 0.65 ± 0.05 wt%. Hereafter, these catalysts are represented as Pd/M-LDH-Z, where M is the intercalated metal cation and Z is the counter anion in the original layered double hydroxide structure.

2.2. Catalyst characterisation

Catalyst surface areas, S_{BET}, were obtained by the BET method from nitrogen physisorption measured at −196 °C on Micromeritics ASAP 2000 instrument. Prior to analysis the samples were outgassed at 250 °C. Water content in the catalysts was determined by thermogravimetric analysis (TGA) using a Perkin Elmer TGA 7 instrument. Samples were heated to 600 °C at a heating rate of 10 °C per minute in air. ICP analysis was conducted on a Spectro Ciros spectrometer. X-ray powder diffraction data were recorded with Cu$K\alpha_1$ radiation on a Stoe Stadi-P diffractometer in either Bragg–Brentano or Debye–Scherrer geometry. Palladium dispersion in the catalysts was determined by hydrogen chemisorption measured by pulse technique using a Micromeritics TPD/TPR 2900 instrument as described elsewhere [26]. Prior to adsorption of H_2, catalyst samples were treated in H_2 flow at 250 °C for 2 h then exposed to air for several hours at room temperature to adsorb oxygen on the Pd surface. The dispersion, D, defined as the fraction of palladium at the surface, $D = Pd_s/Pd_{total}$, was calculated assuming the stoichiometry of H_2 adsorption [27]:

$$Pd_sO + 1.5H_2 \rightarrow Pd_sH + H_2O.$$

Solid-state magic angle spinning (MAS) NMR measurements were conducted at 9.4 T on a Bruker Avance DSX-400 spectrometer equipped with a 4 mm ^{1}H/X/Y CP/MAS probehead using zirconia rotors of 4 mm external diameter. ^{27}Al MAS NMR spectra were acquired at 104.20 MHz using a $\pi/18$ pulse length of 0.40 μs at a MAS rate of 10.0 kHz. The recycle delay was set to 1.0 s and the position of the ^{27}Al resonances is quoted in ppm from external $[Al(H_2O)_6]^{3+}$ (0.1 M aqueous solution of $Al(NO_3)_3$). ^{7}Li MAS NMR spectra were acquired at 155.52 MHz using a $\pi/9$ pulse of 0.60 μs at a MAS rate of 10.0 kHz. The recycle delay was set at 2.0 s and the position of the ^{7}Li resonances is quoted in ppm from external 1 M LiCl aqueous solution.

2.3. Reaction studies

The reactions were performed in the gas phase under atmospheric pressure in a Pyrex glass fixed-bed microreactor (9 mm internal diameter, 0.20 g catalyst bed) as described in detail elsewhere [4]. All gas lines were made of stainless steel. The downstream lines were heated to 150 °C to prevent product condensation. The catalyst was pretreated *in situ* under hydrogen flow at 250 °C for 1 h. The gas mixture (6 ml/min N_2, 4 ml/min H_2 flow rate) was saturated with acetone in a saturator. The molar ratio [acetone]/[H_2] was 5:2 and the contact time 3.0 s. The analysis of products was performed by on-line gas chromatography using a Varian Star 3400CX instrument equipped with a flame ionisation detector and 30 m × 0.25 mm HP-INNOWAX capillary column.

3. Results and discussion

3.1. Characterisation of supports and catalysts

γ-$Al(OH)_3$ was successfully intercalated with a range of metal salts forming intercalation compounds with the composition $[LiAl_2(OH)_6]X{\cdot}nH_2O$ (X = NO_3, OH) or $[MAl_4(OH)_{12}][NO_3]_2{\cdot}nH_2O$ (M = Co, Ni, Cu, Zn) [21,22]. Intercalation was confirmed by powder X-ray diffraction giving phases with interlayer separations of 8.9 Å for $[LiAl_2(OH)_6][NO_3]{\cdot}H_2O$ (see Fig. 1b), 7.4 Å for $[LiAl_2(OH)_6][OH]{\cdot}2H_2O$ and 8.5 Å for $[MAl_4(OH)_{12}][NO_3]_2{\cdot}nH_2O$ (M = Co, Ni, Cu, Zn) in agreement with the literature values. In the case of the nitrate-containing materials, a small amount of unreacted gibbsite (Fig. 1a) remained in the samples as is typically seen for these materials [22]. Additional characterisation of the intercalates was achieved by TGA. A comparison of the TGA traces of

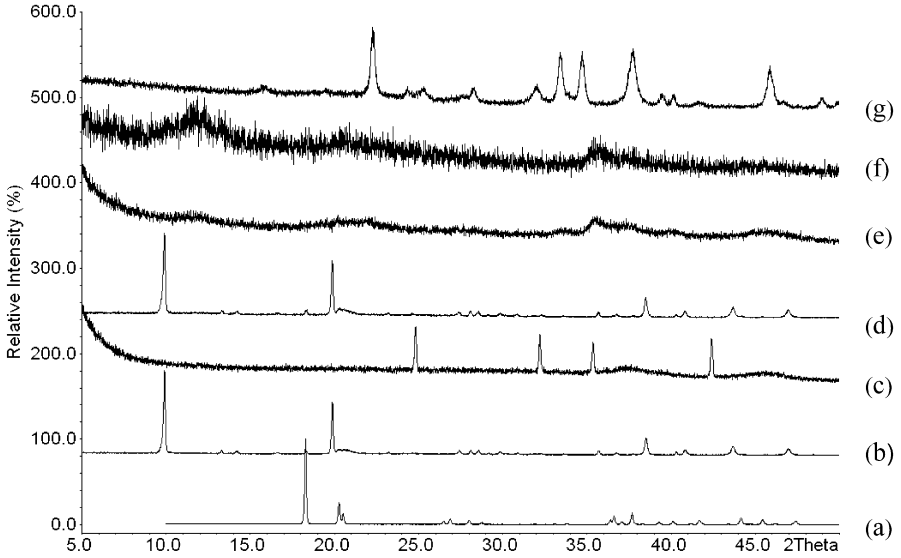

Fig. 1. Powder XRD patterns of (a) gibbsite (γ-Al(OH)$_3$), (b) [LiAl$_2$(OH)$_6$][NO$_3$]·nH$_2$O as synthesised, (c) [LiAl$_2$(OH)$_6$][NO$_3$]·nH$_2$O calcined at 250 °C, (d) fresh Pd(OAc)$_2$/Li-LDH-NO$_3$ prior to reduction and (e) 0.65% Pd/Li-LDH-NO$_3$ after reduction by H$_2$ at 250 °C, (f) 0.65% Pd/Li-LDH-NO$_3$ after use in the gas-phase conversion of acetone to MIBK at 250 °C for 6 h and (g) used 0.65% Pd/Li-LDH-NO$_3$ catalyst after calcination at 1000 °C in air.

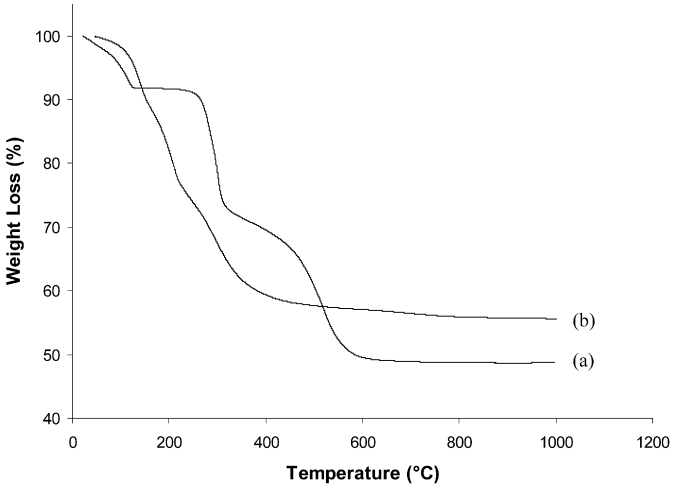

Fig. 2. TGA traces of (a) [LiAl$_2$(OH)$_6$][NO$_3$]·nH$_2$O and (b) [LiAl$_2$(OH)$_6$][OH]·nH$_2$O (heating in N$_2$ with ramp rate 20 °C/min).

[LiAl$_2$(OH)$_6$][NO$_3$]·H$_2$O and [LiAl$_2$(OH)$_6$][OH]·2H$_2$O is shown in Fig. 2. [LiAl$_2$(OH)$_6$][NO$_3$]·H$_2$O displays three mass losses below 650 °C characteristic of LDHs. Initially interlayer water is lost with a mass loss of 8.3% (calculated 7.4%). This is followed by a further mass loss of 23.5% (22.3%) by 350 °C corresponding to the dehydroxylation of the layers and subsequent decomposition to a largely amorphous material with the nominal composition 0.5Li$_2$O + Al$_2$O$_3$ with a mass loss of 20.2% (22.2%). On further heating to 1000 °C in air the crystalline phases LiAl$_5$O$_8$ and LiAlO$_2$ are formed [28]. The [MAl$_4$(OH)$_{12}$][NO$_3$]$_2$·nH$_2$O (M = Co, Ni, Cu, Zn) LDHs exhibited similar decomposition patterns to [LiAl$_2$(OH)$_6$][NO$_3$]·nH$_2$O. In the case of [LiAl$_2$(OH)$_6$][OH]·2H$_2$O the decomposition steps are less distinct but a total mass loss of 44.4% (45.9%) is observed by 600 °C.

The catalysts were prepared by impregnation of the LDHs with Pd(OAc)$_2$. Powder X-ray diffraction patterns of the Pd-doped materials indicate that there is no change in the intercalates during this process (shown in Fig. 1d for [LiAl$_2$(OH)$_6$][NO$_3$]·nH$_2$O) suggesting that there is only surface adsorption of the Pd(OAc)$_2$ and no anion exchange during the pre-treatment process. On subsequent reduction with H$_2$ at 250 °C there is a significant loss of crystallinity in the materials (Fig. 1e) which is consistent with the simultaneous reduction of Pd^{2+} and decomposition of the LDH. It should be noted that calcination of the pristine intercalate at 250 °C leads to the formation of crystalline LiNO$_3$ in addition to the expected poorly crystalline material but this is suppressed in the Pd-doped catalysts [23]. Elemental analysis conducted on [LiAl$_2$(OH)$_6$][NO$_3$]·nH$_2$O and reduced Pd-doped [LiAl$_2$(OH)$_6$][NO$_3$]·nH$_2$O showed almost complete loss of nitrogen from the material upon reduction of the Pd-doped sample at 250 °C for 2 h. This is a further indication of the collapse of the layered structure and formation of a mixed oxide material containing Pd metal. Fig. 1f confirms that there is little bulk structural change of the material during the catalytic process, with crystalline LiAl$_5$O$_8$ and LiAlO$_2$ (and PdO for the doped catalysts) not forming unless the materials are calcined at higher temperatures (Fig. 1g).

^{27}Al MAS NMR of the parent gibbsite material (Fig. 3) yields two resonances at −2.8 and 7.7 ppm which arise from the two crystallographically distinct aluminium sites in gibbsite [28,29]. The ^{27}Al MAS NMR of the as-synthesised [LiAl$_2$(OH)$_6$][NO$_3$]·H$_2$O LDH and this LDH impregnated with palladium acetate, Pd(OAc)$_2$/Li-LDH-NO$_3$, before reduction with H$_2$ are similar showing a single resonance at 8.4 ppm confirming the presence of octahedral Al sites (Fig. 3a). The similarity between these two spectra is consistent with powder XRD results further supporting no change in local structure of the LDH upon doping with Pd(OAc)$_2$. The H$_2$ reduction of the catalyst at 250 °C results in appearance of an additional broad line at ca. 74 ppm attributable to Al sites in tetrahedral coordination along with a broadening of the octahedral Al peak. The used catalyst displays an increased population of tetrahedral Al sites along with an additional narrow resonance at 80.1 ppm. This tetrahedral site may originate from the formation of LiAl$_5$O$_8$ and LiAlO$_2$ phases [28]. These phases become more dominant upon calcination at 1000 °C in air indicated by increased population of tetrahedral Al sites (Fig. 3g). The broadening of both the tetrahedral Al site at 70.0 ppm and octahedral Al site at 7.74 ppm is consistent with powder XRD results showing the deformation of the LDH structure into an amorphous phase. ^{7}Li MAS NMR (see supplementary information) of all the materials showed a single resonance at 0.16 ppm.

Table 1 shows surface areas, S_{BET}, pore volumes and average pore diameters for Pd/LDH catalysts and LDH supports. The as-synthesised LDH materials had low surface areas and pore

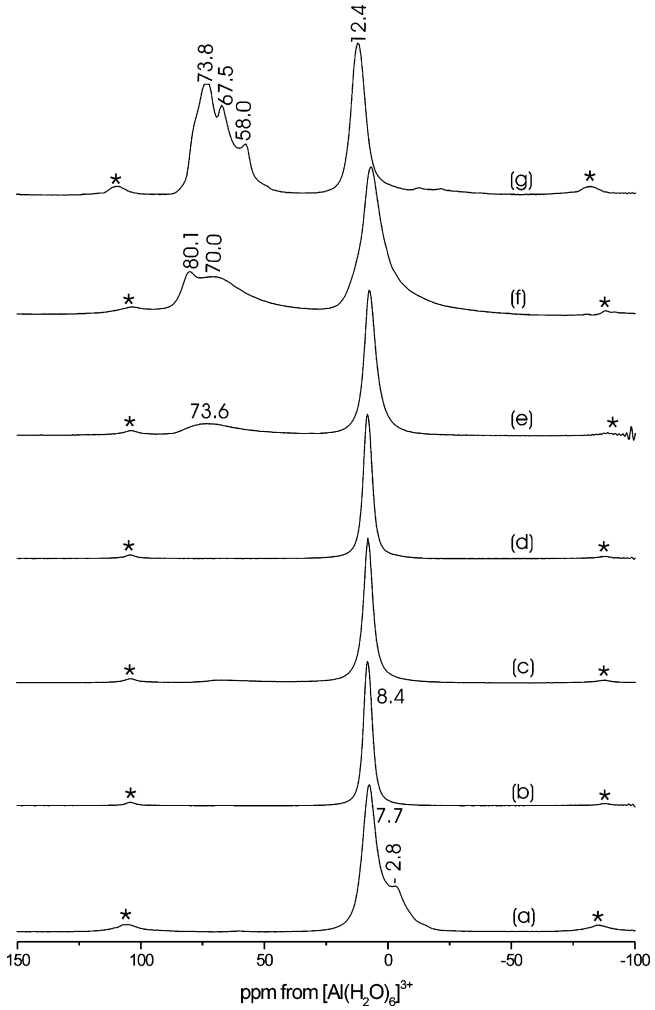

Fig. 3. ^{27}Al MAS NMR spectra of (a) gibbsite, (b) $[LiAl_2(OH)_6][NO_3]\cdot nH_2O$ as synthesised, (c) $[LiAl_2(OH)_6][NO_3]\cdot nH_2O$ after calcination at 250 °C, (d) $Pd(OAc)_2$/Li-LDH-NO_3 as synthesised before reduction with H_2, (e) 0.65% Pd/Li-LDH-NO_3 after reduction with H_2 at 250 °C for 2 h, (f) 0.65% Pd/Li-LDH-NO_3 after use in the gas-phase conversion of acetone to MIBK at 250 °C for 6 h and (g) 0.65% Pd/Li-LDH-NO_3 after use in the gas-phase conversion of acetone to MIBK at 250 °C for 6 h and subsequent calcination at 1000 °C in air. Asterisks denote spinning side bands.

volumes. The reduction of the LDHs at 250 °C results in a significant increase in the surface area and pore volume due to collapse of their structure. For example, the surface area for $[ZnAl_4(OH)_{12}][NO_3]_2\cdot nH_2O$ increased from 6 to 210 m^2/g after the reduction. The surface area for Pd catalysts that were all treated by H_2 at 250 °C ranged from 76 to 341 m^2/g.

The dispersion of Pd in the catalysts, D, as obtained from H_2 chemisorption, is shown in Table 1. It should be noted that in the absence of palladium the LDH materials did not adsorb hydrogen. The dispersion of Pd in the catalysts prepared from Li-LDH and gibbsite which did not contain reducible metal ions ranged from 0.12–0.43. Pd/Zn-LDH-NO_3 with $D = 0.40$ also fell in this range. A disproportionally large dispersion of 2.35 for Pd/Co-LDH-NO_3 indicates reduction of Co^{2+} to Co metal in the catalyst, with the latter contributing to H_2 adsorption. Also a relatively large dispersion for Pd/Ni-LDH-NO_3 ($D = 0.58$) might partly be due to the presence of Ni metal in the catalyst.

3.2. Catalyst testing

The gas-phase synthesis of MIBK was studied in a fixed-bed flow reactor under the following conditions: 120–300 °C, ambient pressure, 3.0 s contact time (GHSV of 1200 h^{-1}) and a volume ratio [acetone]:[H_2]:[N_2] = 50:20:30 in the gas feed. The Pd loading on the catalysts was 0.65 wt%. Prior to use, the catalysts were pretreated *in situ* in hydrogen flow at 250 °C for 1 h.

Table 1
Catalyst texture and Pd dispersion[a]

Catalyst	S_{BET} (m^2/g)	Pore diameter[b] (Å)	Pore volume[c] (cm^3/g)	D[d]
$[LiAl_2(OH)_6][NO_3]\cdot nH_2O$[e]	7	81	0.01	
0.65% Pd/Li-LDH-NO_3	131	88	0.29	0.19
0.65% Pd/Li-LDH-OH	76	83	0.16	0.12
0.65% Pd/Co-LDH-NO_3	266	36	0.19	2.35[f]
0.65% Pd/Cu-LDH-NO_3	130	26	0.08	
$[ZnAl_4(OH)_{12}][NO_3]_2\cdot nH_2O$[e]	6	72	0.01	
Zn-LDH-NO_3	210	25	0.13	
0.65% Pd/Zn-LDH-NO_3	262	26	0.17	0.40
0.65% Pd/Ni-LDH-NO_3	341	34	0.29	0.58
0.65% Pd/$Al(OH)_3$	328	24	0.19	0.43

[a] All catalysts were treated at 250 °C in H_2 for 2 h unless stated otherwise.
[b] Average pore diameter by BET.
[c] Single point total pore volume.
[d] Palladium dispersion: $D = Pd_s/Pd_{total}$.
[e] LDH materials as prepared without treatment in H_2 at 250 °C.
[f] Disproportionately large dispersion indicates reduction of Co^{2+} to Co metal.

Table 2
Acetone conversion and reaction selectivity at 120 °C (3 h on stream)

Catalyst	Conv. (%)	Selectivity (%)[a]					
		C_3	IP	MIBK	DIBK	MO	Others
Li-LDH-NO_3	0.3	Trace	0	Trace	0	~60	Trace
0.65% Pd/Li-LDH-NO_3	20.0	0.2	7.5	70.0	16.1	0.3	6.0
0.65% Pd/Li-LDH-OH	15.5	0.3	33.6	54.2	8.5	2.8	0.6
Co-LDH-NO_3	5.4	Trace	0	Trace	0	~90	Trace
0.65% Pd/Co-LDH-NO_3	21.6	0.4	82.0	15.4	0.4	1.7	0
0.65% Pd/Cu-LDH-NO_3	23.4	0.4	74.3	22.5	0.9	1.9	0
Zn-LDH-NO_3	2.4	Trace	0	Trace	0	~80	3.3
0.65% Pd/Zn-LDH-NO_3	20.2	0.2	22.9	63.2	8.9	4.0	0.9
Ni-LDH-NO_3	3.5	Trace	0	0	0	~90	Trace
0.65% Pd/Ni-LDH-NO_3	26.5	0.3	67.3	28.4	1.5	2.5	0.1
0.65% Pd/$Al(OH)_3$	12.9	0.5	46.5	48.8	0.7	3.1	0.4

[a] C_3 is propane and propene, IP isopropanol, MO mesityl oxide, others mainly C_{9+} condensation products and mesitylene.

Representative results at 120 °C are given in Table 2. The reaction clearly required both acid–base and hydrogenation catalysis which was provided by a mixed oxide derived from LDHs and Pd, respectively. When the mixed oxides were used in the absence of Pd, the conversion of acetone was very low (0.3–3.4%), and mesityl oxide (the product of acid–base catalysed condensation of acetone) was the major product (60–90% selectivity), with only traces of MIBK formed. This shows that the mixed oxides themselves, even those containing Ni and Co, acted as acid–base catalysts, with a very weak hydrogenation activity.

In the presence of Pd-doped catalysts, acetone conversion increased up to 26% (Table 2). The Pd catalysts originated from Li-LDH and Zn-LDH gave MIBK as the major reaction product (up to 70% selectivity), with significant amount of DIBK also formed. Reaction by-products included isopropanol (IP), mesityl oxide (MO), C_{9+} acetone condensation products (mainly the tetramer 2,6,8-trimethylnonane-4-one together with mesitylene) and small amounts ($\leqslant$1% selectivity) of propene and propane (C_3). In contrast, the catalysts obtained from transition metal (Cu, Ni and Co) LDHs gave isopropanol as the major product by direct hydrogenation of acetone, with up to 82% IP selectivity for Pd/Co-LDH-NO_3. This may be explained by the presence of Cu, Ni and Co metal particles in these catalysts, as mentioned above, which could catalyse hydrogenation of the C=O group in acetone. Palladium supported on gibbsite, γ-$Al(OH)_3$, exhibited relatively weak activity, yielding an almost equal amount of MIBK and IP, which shows that

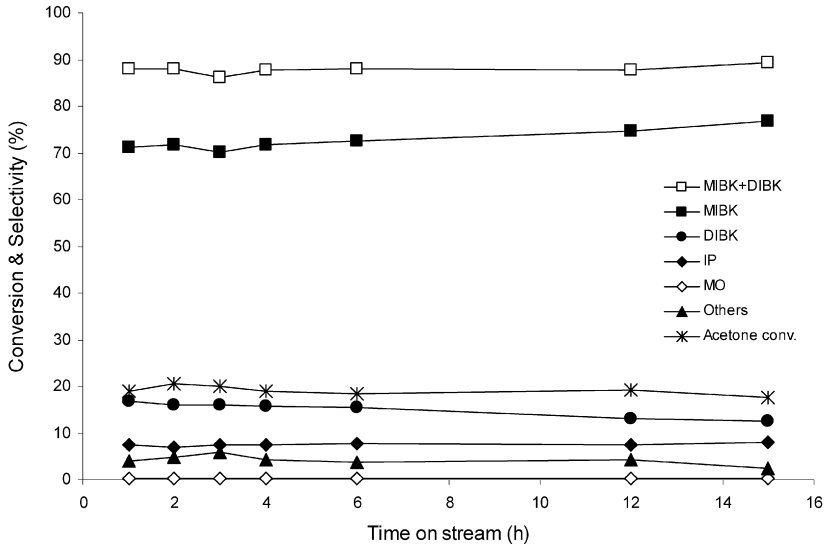

Fig. 4. Acetone conversion and product selectivity vs time on stream (Pd/Li-LDH-NO_3, 120 °C).

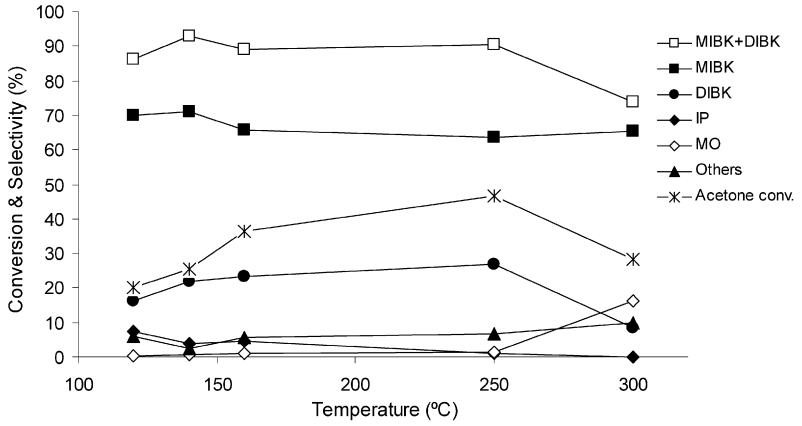

Fig. 5. Acetone conversion and product selectivity vs reaction temperature (Pd/Li-LDH-NO_3, 3 h time on stream).

the second metal cation in LDH plays an important role, enhancing catalyst performance. It should be pointed out that there was no relation between catalyst performance (catalysts activity and selectivity) at 120 °C and the Pd dispersion (Table 1).

Pd/Li-LDH-NO_3 was the most efficient catalyst at 120 °C, giving 70% MIBK selectivity and 86% MIBK + DIBK combined selectivity at 20% acetone conversion. This catalyst also exhibited very good stability (Fig. 4). No catalyst deactivation was observed during at least 15 h continuous operation. The catalyst reached steady state in about 1 h and after that performed with a constant activity and selectivity.

Increasing the reaction temperature up to 250 °C led to an increase in acetone conversion, with MIBK and DIBK selectivities almost unchanged (Fig. 5). However, further temperature ramp to 300 °C caused a drop in catalyst activity probably because of a structural change in the catalyst due to its dehydration.

Table 3 shows catalyst performance at the optimal temperature of 250 °C. At this temperature, high acetone conversions were obtained, up to 77%. For all the catalysts studied, MIBK was the major product (47–91% selectivity), with large MIBK + DIBK combined selectivities from 82 to 98%. This compares well with the results reported previously [2–7,15–20,30]. In contrast to the results at 120 °C (Table 2), the catalysts containing Co and Ni with the largest surface areas of 266 and 341 m^2/g respectively (Table 1), were amongst the most active ones at 250 °C, followed by Pd/Zn-LDH-NO_3 ($S_{BET} = 262\ m^2/g$). At this temperature, the catalysts with higher metal dispersions exhibited higher catalytic activities. Pd/Co-LDH-NO_3 showed the highest activity (77% conversion), with the largest MIBK yield of 44% and MIBK + DIBK combined yield of 69%. Pd/Li-LDH-OH gave the highest MIBK selectivity of 91% and MIBK + DIBK selectivity of 98%, although at a low acetone conversion of 15%.

Table 3
Acetone conversion and reaction selectivity at 250 °C (3 h on stream)

Catalyst	Conv. (%)	Selectivity (%)[a]					
		C_3	IP	MIBK	DIBK	MO	Others
0.65% Pd/Li-LDH-NO_3	46.8	0	1.2	63.6	27.0	1.5	6.6
0.65% Pd/Li-LDH-OH	15.1	0.3	0	90.9	7.2	0.4	1.3
0.65% Pd/Co-LDH-NO_3	76.5	0.7	2.2	57.9	32.6	1.3	5.4
0.65% Pd/Cu-LDH-NO_3	37.7	7.9	3.5	60.9	20.9	1.6	5.2
0.65% Pd/Zn-LDH-NO_3	67.2	2.9	2.3	53.5	30.5	1.3	9.6
0.65% Pd/Ni-LDH-NO_3	72.2	0.9	3.8	47.2	36.9	1.4	9.8

[a] C_3 is propane and propene, IP—isopropanol, MO—mesityl oxide, others—mainly C_{9+} condensation products and mesitylene.

The catalysts exhibited fairly good stability at 250 °C, as exemplified by the results for Pd/Ni-LDH-NO_3 over 18 h on stream (Fig. 6). The catalyst reached steady state in about 2 h and after that performed at a constant MIBK + DIBK selectivity, showing a slow decrease in acetone conversion from 73 to 60% in 16 h. In this

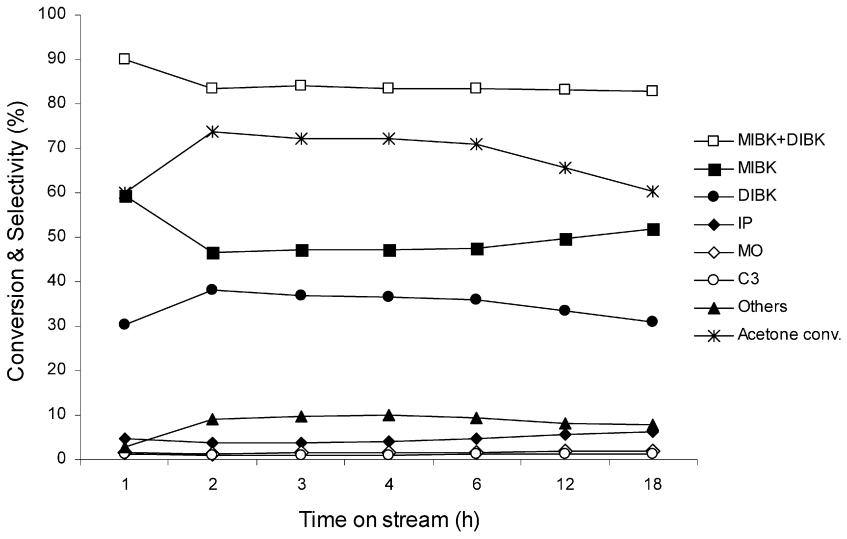

Fig. 6. Acetone conversion and product selectivity vs time on stream (Pd/Ni-LDH-NO_3, 250 °C).

run, the MIBK selectivity was increasing at the expense of DIBK, as expected for consecutive products.

4. Conclusion

Pd-doped novel intercalated layered double hydroxides derived from gibbsite have proven to be precursors to efficient bifunctional mixed oxide catalysts for the one-step conversion of acetone to MIBK in the gas phase. An MIBK selectivity of 70% (86% total MIBK + DIBK selectivity) at an acetone conversion of 20% was achieved using the 0.65 wt% Pd/Li-LDH-NO_3 at a low reaction temperature of 120 °C and atmospheric pressure, without catalyst deactivation for at least 15 h on stream. At the optimum reaction temperature of 250 °C, high acetone conversions of up to 77% with 91% combined MIBK + DIBK selectivity and fairly good catalyst stability were achieved. Initially crystalline LDHs transformed to amorphous mixed oxide materials upon catalysts activation at 250 °C under H_2.

Acknowledgments

We would like to thank EPSRC for DTA awards (R.D.H., R.M. and J.T.A.J.). A.M.F. thanks the Royal Society for a University Research Fellowship.

Supplementary information

Supplementary information for this article may be found on ScienceDirect, in the online version.

Please visit DOI: 10.1016/j.jcat.2008.06.017.

References

[1] K. Weissermel, H.-J. Arpe, Industrial Organic Chemistry, third ed., VCH, Weinheim, 1997, p. 280.
[2] F. Delbecq, P. Sautet, J. Catal. 152 (1995) 217.
[3] R.D. Hetterley, E.F. Kozhevnikova, I.V. Kozhevnikov, Chem. Commun. (2006) 782.
[4] E.F. Kozhevnikova, I.V. Kozhevnikov, J. Catal. 238 (2006) 286.
[5] P.Y. Chen, N.S. Chang, T.K. Chuang, L.Y. Chen, Stud. Surf. Sci. Catal. 46 (1989) 230.
[6] C.O. Veloso, J.L.F. Monteiro, E.F. Sousaaguiar, Stud. Surf. Sci. Catal. 84 (1994) 1913.
[7] S.M. Yang, Y.M. Wu, Appl. Catal. A 192 (2000) 211.
[8] F. Cavani, F. Trifiro, A. Vaccari, Catal. Today 11 (1991) 173.
[9] B.F. Sels, D.E. De Vos, P.A. Jacobs, Catal. Rev.-Sci. Eng. 43 (2001) 443.
[10] S. Miyata, T. Kumura, Chem. Lett. 8 (1973) 843.
[11] A.I. Khan, D. O'Hare, J. Mater. Chem. 12 (2002) 3191.
[12] G.R. Williams, D. O'Hare, J. Mater. Chem. 16 (2006) 3065.
[13] R. Allman, Chimia 24 (1970) 99.
[14] W.T. Reichle, J. Catal. 94 (1985) 547.
[15] R. Unnikrishnan, S. Narayanan, J. Mol. Catal. A 144 (1999) 173.
[16] N. Das, D. Tichit, R. Durand, P. Graffin, B. Coq, Catal. Lett. 71 (2001) 181.
[17] M. Martinez-Ortiz, D. Tichit, P. Gonzalez, B. Coq, J. Mol. Catal. A 201 (2003) 199.
[18] N.N. Das, S.C. Srivastava, Bull. Mater. Sci. 25 (2002) 283.
[19] A.A. Nikolopoulos, B.W.L. Jang, J.J. Spivey, Appl. Catal. A 296 (2005) 128.
[20] F. Winter, A.J. van Dillen, K.P. de Jong, J. Mol. Catal. A 219 (2004) 273.
[21] A.V. Besserguenev, A.M. Fogg, R.J. Francis, S.J. Price, D. O'Hare, V.P. Isupov, B.P. Tolochko, Chem. Mater. 9 (1997) 241.
[22] A.M. Fogg, G.R. Williams, R. Chester, D. O'Hare, J. Mater. Chem. 14 (2004) 2369.
[23] K.R. Poeppelmeier, S.J. Hwu, Inorg. Chem. 26 (1987) 3297.
[24] A.M. Fogg, D. O'Hare, Chem. Mater. 11 (1999) 1771.
[25] G.R. Williams, T.G. Dunbar, A.J. Beer, A.M. Fogg, D. O'Hare, J. Mater. Chem. 16 (2006) 1222.
[26] M. Musawir, E.F. Kozhevnikova, I.V. Kozhevnikov, J. Mol. Catal. A 262 (2007) 93.
[27] J.E. Benson, H.S. Hwang, M. Boudart, J. Catal. 30 (1973) 146.
[28] X.Q. Hou, Inorg. Chem. 40 (2001) 6397.
[29] H. Saalfeld, Z. Kristallogr. 139 (1974) 129.
[30] D. Tichit, C. Gerardin, R. Durand, B. Coq, Top. Catal. 39 (2006) 89.